Firefly luciferase mutants as sensors of proteome stress

Rajat Gupta[1], Prasad Kasturi[1], Andreas Bracher[1], Christian Loew[1], Min Zheng[1], Adriana Villella[2], Dan Garza[2], F Ulrich Hartl[1,3] & Swasti Raychaudhuri[1]

Maintenance of cellular protein homeostasis (proteostasis) depends on a complex network of molecular chaperones, proteases and other regulatory factors. Proteostasis deficiency develops during normal aging and predisposes individuals for many diseases, including neurodegenerative disorders. Here we describe sensor proteins for the comparative measurement of proteostasis capacity in different cell types and model organisms. These sensors are increasingly structurally destabilized versions of firefly luciferase. Imbalances in proteostasis manifest as changes in sensor solubility and luminescence activity. We used EGFP-tagged constructs to monitor the aggregation state of the sensors and the ability of cells to solubilize or degrade the aggregated proteins. A set of three sensor proteins serves as a convenient toolkit to assess the proteostasis status in a wide range of experimental systems, including cell and organism models of stress, neurodegenerative disease and aging.

Proteins are involved in virtually every biological process. The failure of proteins to fold or to maintain their folded states may result in the loss of essential functions and the formation of toxic aggregates[1,2]. Thus, quality control and the maintenance of protein homeostasis (proteostasis) are critical for cell and organism health. In multicellular organisms, proteostasis is achieved and controlled by a complex network of several hundred dedicated proteins, including molecular chaperones and their regulators[2,3] as well as the ubiquitin-proteasome and autophagy systems[1,4]. Deficiencies in proteostasis are associated with many diseases, such as metabolic disorders, neurodegeneration, cancer and cardiovascular disease. A major risk factor of these diseases is age. Indeed, recent studies in model organisms indicate that the aging process is linked to a decline in cellular proteostasis capacity[5]. As a result, the proteostasis network is emerging as an attractive target for pharmacological intervention in age-related disorders[1,6,7].

Understanding the function and regulation of the proteostasis network requires molecular tools to measure its activity status, so-called proteostasis sensors. Pioneering studies in *Caenorhabditis elegans* had used temperature-sensitive mutant proteins as proteostasis sensors. These mutations manifest in a phenotype at the permissive temperature upon expression of aggregating Huntington's disease protein or during normal aging[5,8]. However, these proteins have some limitations as proteostasis sensors. Their compromised folding may lead to loss-of-function effects and reduced viability. Moreover, tissue-specific mutant phenotypes may complicate the comparative analysis of different cell types and organs. To circumvent these limitations, we developed proteostasis sensor proteins with varying conformational stability derived from luciferase. This protein has no known biological role in widely used cellular and animal models, and thus the sensors can be used with minimal perturbation of the system under investigation.

To generate sensitive reporters of proteostasis capacity, we selected the American firefly (*Photinus pyralis*) luciferase (Fluc), a ~60 kDa multidomain protein known to be chaperone-dependent for folding and refolding[9–12]. The monomeric functional unit of this protein does not require post-translational modification[13]. Fluc activity can be measured by a luminescence-based assay with exquisite sensitivity and a wide dynamic range in cell extracts, intact cells and model organisms[14]. Indeed, Fluc has been used previously to compare intraorganellar chaperone capacities[15,16]. Here we describe increasingly conformationally destabilized variants of Fluc (with fused enhanced GFP (EGFP)), which require chaperone surveillance to maintain their soluble, enzymatically active state. These proteins serve as sensors of proteostasis capacity in different cell lines and in *C. elegans* under stress conditions, during aging or upon treatment with proteostasis-modifying compounds.

RESULTS

Conformationally destabilized Fluc mutants

Fluc consists of two domains[13] (**Fig. 1a**). The active-site pocket for the substrates, ATP and luciferin, is located in the large N-terminal domain (residues 1–421). The C-terminal domain (residues 422–544) serves as a lid over the active site and is thought to seal the excited-state oxyluciferin, the product of the enzymatic reaction, from solvent-mediated quenching of luminescence[13]. Although Fluc is normally located in firefly peroxisomes,

[1]Department of Cellular Biochemistry, Max Planck Institute of Biochemistry, Martinsried, Germany. [2]Proteostasis Therapeutics Inc., Cambridge, Massachusetts, USA. [3]Center for Integrated Protein Science, München, Germany. Correspondence should be addressed to F.U.H. (uhartl@biochem.mpg.de) or S.R. (raychaud@biochem.mpg.de).

RECEIVED 2 MARCH; ACCEPTED 26 JULY; PUBLISHED ONLINE 4 SEPTEMBER 2011; DOI:10.1038/NMETH.1697

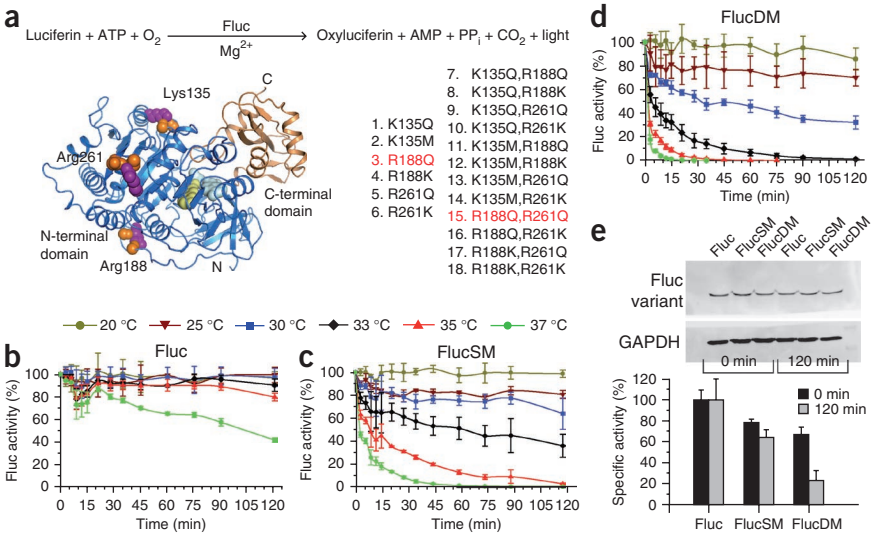

Figure 1 | Thermal stability of luciferase sensor proteins. (**a**) Fluc-mediated enzymatic reaction and Fluc crystal structure (Protein Data Bank: 2d1r)[26]. Highlighted are N-terminal domain (blue) and C-terminal domain (gold) as well as mutated residues (pink) and their hydrogen bond interactors (orange; Asp107 and Tyr109, Glu18 and Gly20, and Thr43 and Asn50). Bound enzyme products AMP and oxyluciferin are shown in light blue and light green van-der-Waals envelopes, respectively. Generated mutations are listed, with those discussed in the paper shown in red. (**b**–**d**) Temperature-dependent Fluc activity of Fluc (**b**), FlucSM (**c**) and FlucDM (**d**) measured at the indicated times and expressed as a percentage of the activity measured immediately after translation (set to 100%). Proteins were translated in reticulocyte lysate (90 min at 30 °C), followed by inhibition of translation and incubation at 20–37 °C. Error bars, s.d.; $n = 3$. (**e**) Specific luminescence activity of Fluc, FlucSM and FlucDM immediately after translation and after 2 h of incubation at 30 °C (bottom). Amounts of Fluc variants were determined by immunoblotting of total reticulocyte lysate fractions (top) compared to GAPDH control and densitometry. Specific activity of wild-type Fluc was set to 100%. Error bars, s.d.; $n = 3$.

it remains mainly in the cytosol when expressed in mammalian cells, as the capacity for uptake into peroxisomes is limited (Sherf, B.A. & Wood, K.V. Firefly luciferase engineered for improved genetic reporting. Promega Notes 49, 14; 1994). We nevertheless replaced the C-terminal peroxisome-targeting signal, Ser-Lys-Leu, by Ile-Ala-Val to avoid import into peroxisomes.

To design increasingly destabilized mutants of Fluc with unchanged enzymatic activity in the folded state, we mutated the N-terminal domain to weaken polar contacts between amino acids that are located far apart in the luciferase sequence; such interactions often contribute substantially to the thermodynamic stability of the native fold[17]. We excluded mutations close to the substrate-binding pocket as well as mutations at the domain-domain interface to maintain the high quantum yield of the luminescence reaction. We chose Lys135, Arg188 and Arg261for mutagenesis, which are within hydrogen bond distance to Asp107 and Tyr109, Glu18 and Gly20, and Thr43 and Asn50, respectively. Using this strategy, we generated 6 single mutants and 12 double mutants of Fluc (**Fig. 1a**).

To test the conformational and functional stability of the Fluc mutants, we translated the proteins *in vitro* in rabbit reticulocyte lysate at 30 °C. After terminating translation, we incubated the reaction mixtures at different temperatures and measured luciferase activities. Wild-type Fluc retained ~40% of the original enzymatic activity after 2 h at 37 °C and was stable up to 35 °C (**Fig. 1b**). The single mutants were generally less stable, losing >90% of activity in 60 min at 37 °C and 50–80% at 35 °C but maintained stable activity up to 33 °C (**Fig. 1c** and **Supplementary Fig. 1a**). The Fluc(R188Q) single mutant examined in this work in detail, here referred to as FlucSM, had substantial instability already at 30 °C and 33 °C (**Fig. 1c**). As expected, the Fluc double mutants were destabilized relative to the single mutants from which they were derived, losing 80% of the original activity within 5 min of incubation at 37 °C and 20 min at 35 °C (**Fig. 1d** and **Supplementary Fig. 1b**). At 33 °C, the double mutants containing R188Q lost 80% of the original activity within 30–40 min (**Fig. 1d** and **Supplementary Fig. 1b**). The double mutant we examined in detail was Fluc(R188Q,R261Q), referred to here as FlucDM.

Immediately after *in vitro* translation, the specific activities (activities relative to protein amount) of FlucSM and FlucDM were 70–80% of the specific activity of Fluc (**Fig. 1e**), indicating that the initial folding of the mutant proteins was highly efficient. In contrast to Fluc, however, the specific activities of FlucSM and FlucDM decreased by ~15% and ~70%, respectively, upon incubation for 2 h at 30 °C, although the proteins remained stable and soluble (**Fig. 1e** and data not shown). We observed very similar behavior for the corresponding Fluc-EGFP variants (**Supplementary Fig. 2**). To confirm that time-dependent loss of enzymatic activity of Fluc mutants was due to increased structural flexibility, we measured the sensitivity of the newly translated proteins to proteinase K. Compared to control reactions without protease, luciferase activity decreased with a half-time ($t_{1/2}$) of ~20 min for FlucSM and ~7 min for FlucDM, whereas Fluc remained stable upon treatment with protease (**Supplementary Fig. 3a**). Digestion profiles of the full-length proteins, as detected by immunoblotting, corresponded to a loss of enzymatic activity (**Supplementary Fig. 3**).

Fluc mutants were thermolabile *in vivo*

To assess the conformational stability of Fluc variants *in vivo*, we first analyzed their behavior in HeLa cells. We transiently expressed Fluc, FlucSM and FlucDM or the corresponding EGFP fusion constructs at low levels (~2.5 µg luciferase protein per milligram total cell protein; **Supplementary Fig. 4**). Compared to Fluc, the specific activity of FlucSM and FlucDM (at 37 °C) was lower by ~40% and 60%, respectively (**Fig. 2a**), suggesting that a large fraction of the mutant protein was misfolded. As expected, RNAi-mediated downregulation (by 50–70%) of Hsc70, a major constitutive chaperone required for Fluc folding[9], compromised the folding efficiency of Fluc and Fluc mutants (**Fig. 2a**).

Next, we analyzed the thermal stability of the sensor proteins under heat stress. In these and all following experiments we used EGFP-tagged Fluc variants. When expressed at 37 °C, all three variants displayed a diffuse cytosolic distribution and some nuclear staining. We observed a small number of green fluorescent

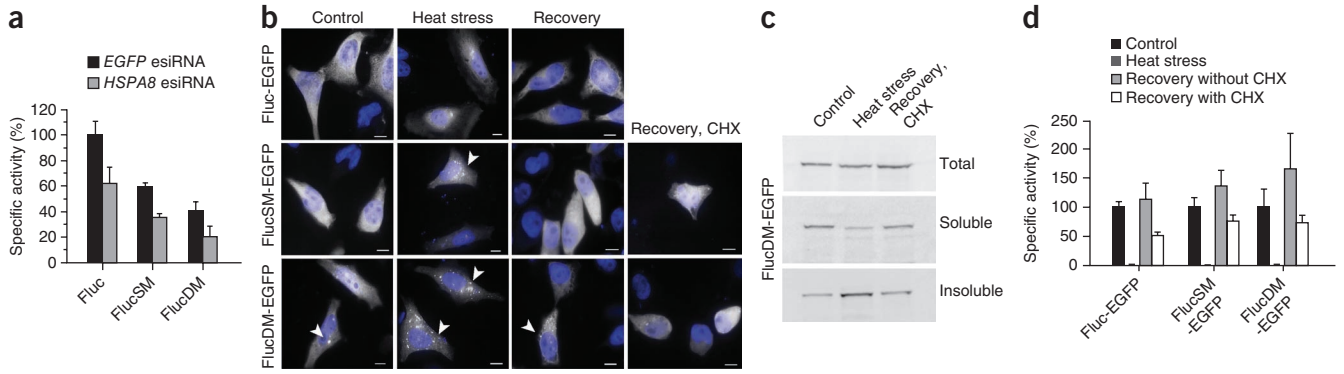

Figure 2 | Chaperone dependence and thermal stability of sensor proteins in HeLa cells. (**a**) To test dependence of Fluc activity on Hsc70, Fluc, FlucSM and FlucDM were expressed for 48 h in cells treated with control endoribonuclease-prepared small interfering (esi)RNA to *EGFP* or esiRNA to *HSPA8* (which encodes Hsc70). Specific activities in soluble extracts are shown relative to that of wild-type Fluc in control cells (set to 100%). Error bars, s.d.; $n = 3$. (**b**) Representative fluorescence micrographs of HeLa cells expressing Fluc-EGFP, FlucSM-EGFP or FlucDM-EGFP subjected to heat stress for 2 h at 43 °C or maintained at 37 °C (control), followed by recovery for 2 h at 37 °C with or without cycloheximide (CHX). EGFP fluorescence (white) was monitored (aggregates are marked by arrowheads). Nuclei were stained with DAPI (blue). Scale bars, 10 µm. (**c**) Cell-fractionation experiment showing total cell extract, detergent-soluble and insoluble fraction of FlucDM-EGFP–expressing HeLa cells treated as in **b**. FlucDM-EGFP was detected by immunoblotting with an antibody to GFP. (**d**) Specific Fluc activity of EGFP-tagged sensor proteins upon heat stress and recovery. HeLa cells expressing Fluc-EGFP variants were treated as in **b**. Specific activities in control cells maintained at 37 °C were set to 100%. Error bars, s.d.; $n = 3$.

'aggregates' in FlucDM-EGFP–expressing cells (**Fig. 2b**). Heat shock at 43 °C for 2 h did not alter the cellular distribution of Fluc-EGFP, but ~45% of the FlucSM-EGFP–expressing cells and ~75% of the FlucDM-EGFP–expressing cells accumulated aggregates. The proteins were increasingly insoluble under these conditions, as shown for FlucDM-EGFP (**Fig. 2c**). Upon recovery from heat shock for 2 h at 37 °C, only 15–20% of FlucSM-EGFP–expressing cells and about 30% of FlucDM-EGFP–expressing cells retained visible aggregates (**Fig. 2b**), suggesting that dissociation or degradation of aggregates had occurred. To exclude the contribution of newly synthesized protein to this process, we added cycloheximide to the cells immediately after heat shock to inhibit translation. Upon recovery of cells from heat shock, we again observed increased diffuse staining of the mutant proteins (**Fig. 2b**). Cell fractionation revealed a greater amount of soluble FlucDM-EGFP (**Fig. 2c**), suggesting dissociation of aggregates. Although we detected essentially no Fluc activity in cell lysates immediately after heat shock, owing to denaturation[18], 50–70% of all Fluc variants renatured during recovery in the presence of cycloheximide (**Fig. 2d**). During recovery in the absence of cycloheximide, the specific activities of all Fluc variants exceeded those in control cells before heat shock (**Fig. 2d**). This effect may be attributed to upregulation of chaperones resulting in increased folding efficiency of newly synthesized protein. Thus, the Fluc-based sensors functioned as reporters of heat stress and allowed assessment of cell capacity to refold heat-denatured protein.

Effect of Fluc mutants on proteostasis

Ideally, sensor proteins should not affect the proteostasis capacity of the cellular system under study. To address this possibility, we expressed the EGFP-tagged sensors in HeLa cells that we also transfected with a reporter for cytosolic stress protein transcription, the structurally unrelated *Renilla reniformis* luciferase (Rluc) under regulation of the stress-sensitive *HSPA1A* promoter. Co-transfection efficiency was ~70% (**Supplementary Fig. 5** and data not shown). Heat-stress treatment of control cells (2 h at 43 °C) resulted in an about tenfold induction of Rluc activity and a corresponding increase in Rluc protein upon immunoblotting, as measured after 2 h of recovery at 37 °C (**Fig. 3**). In contrast, expression of the Fluc variants at 37 °C without heat stress caused only a 1.5–2-fold induction of Rluc activity. This effect was most notable with Fluc-EGFP, which was more highly expressed than FlucSM-EGFP and FlucDM-EGFP (**Fig. 3b**). Thus, low-level expression of the mutant proteins alone caused only a very mild activation of the cytosolic stress response. We observed an about tenfold increase in Rluc activity when we combined expression of Fluc-EGFP variants with heat treatment, indicating that the cells expressing the sensors respond normally to heat stress (**Fig. 3a**). We obtained similar results with non–EGFP-tagged sensor proteins (**Supplementary Fig. 6**).

We next performed experiments in *Drosophila melanogaster* S2 cell lines to determine whether the sensor proteins induce a stress response when expressed at higher levels. S2 cells grow

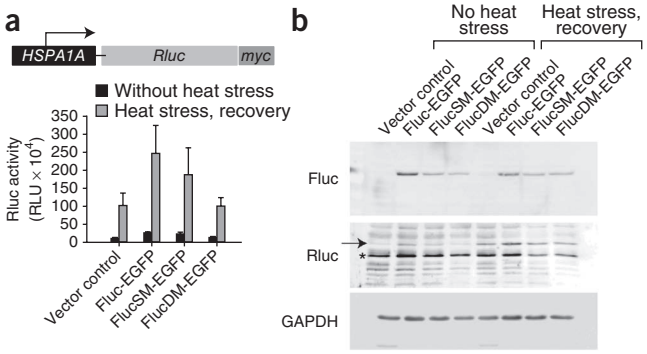

Figure 3 | Effect of Fluc-based sensors on the cytosolic stress response. (**a**) HeLa cells were transfected with the stress-responsive *HSPA1A-Rluc* reporter (top) along with the vectors encoding Fluc-EGFP variants or vector-only control. Rluc activity was measured either without stress or after subjecting the cells to heat stress for 2 h at 43 °C and recovery for 2 h at 37 °C. Error bars, s.d.; $n = 3$. RLU, relative luminiscence unit. (**b**) Amounts of stress-responsive Rluc and Fluc-EGFP variants in HeLa cells treated as in **a**, detected by immunoblotting. GAPDH was used as a loading control. Asterisk indicates a nonspecific band.

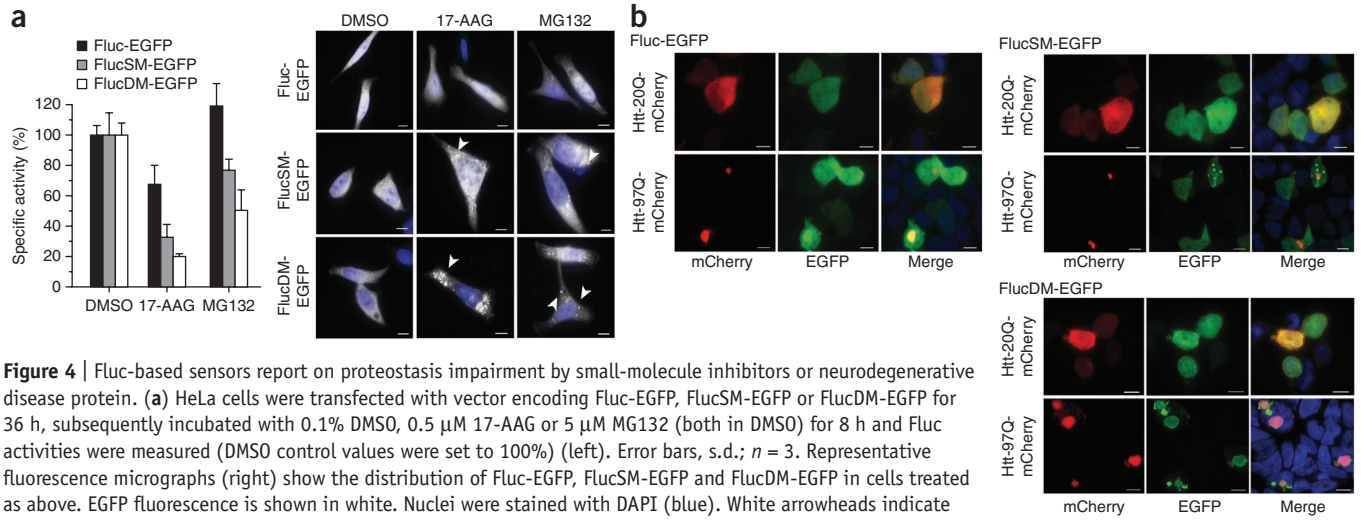

Figure 4 | Fluc-based sensors report on proteostasis impairment by small-molecule inhibitors or neurodegenerative disease protein. (**a**) HeLa cells were transfected with vector encoding Fluc-EGFP, FlucSM-EGFP or FlucDM-EGFP for 36 h, subsequently incubated with 0.1% DMSO, 0.5 μM 17-AAG or 5 μM MG132 (both in DMSO) for 8 h and Fluc activities were measured (DMSO control values were set to 100%) (left). Error bars, s.d.; $n = 3$. Representative fluorescence micrographs (right) show the distribution of Fluc-EGFP, FlucSM-EGFP and FlucDM-EGFP in cells treated as above. EGFP fluorescence is shown in white. Nuclei were stained with DAPI (blue). White arrowheads indicate aggregates. (**b**) Fluorescence micrographs of HEK293T cells 48 h after transfection with vectors encoding Fluc-EGFP variants and *mCherry*-tagged *Htt* exon 1 constructs encoding proteins with 20Q or 97Q. Nuclei were stained with DAPI. All scale bars, 10 μm.

at 25 °C and can express recombinant proteins. We prepared copper-inducible, stable S2 lines expressing the different Fluc variants. Under non-induced conditions, we observed low basal expression of Fluc and Fluc mutants, which did not result in Hsp70 upregulation. However, medium-level overproduction of the mutant proteins (to > tenfold basal level) caused a substantial induction of Hsp70, whereas to achieve similar Hsp70 induction by Fluc required massive overexpression at high copper concentration (**Supplementary Fig. 7**). In conclusion, upon high-level expression, Fluc mutants induced a cytosolic stress response, but at low levels, they perturbed proteostasis only to a limited extent.

Impairment of proteostasis by small-molecule inhibitors

Small-molecule compounds can be used to modulate cellular proteostasis capacity. To test whether the Fluc-based sensors can report such changes, we expressed the proteins in HeLa cells for 36 h and then treated the cells with 0.5 μM of the Hsp90 inhibitor 17-allylamino-17-demethoxygeldanamycin (17-AAG)[19] for 8 h. Hsp90 is a major cytosolic chaperone[20] and is required for the reactivation of Fluc upon recovery from heat stress[18]. Treatment of HeLa cells with 17-AAG reduced the specific activity of Fluc-EGFP, FlucSM-EGFP and FlucDM-EGFP at 37 °C by ~40%, ~60% and more than ~80%, respectively (**Fig. 4a**). We detected small green-fluorescent aggregates in ~8% of cells expressing FlucSM-EGFP, whereas ~50% of cells expressing FlucDM-EGFP accumulated multiple larger aggregates. In contrast, Fluc-EGFP–expressing cells had diffuse cytosolic distribution of fluorescence upon 17-AAG treatment (**Fig. 4a**). Thus, inhibition of Hsp90 compromised the proteostasis system, resulting in partial aggregation of the mutant Fluc-EGFP sensors.

Proteome stress is also induced by inhibiting proteasomal degradation. Treatment with the proteasome inhibitor MG132 (5 μM for 8 h)[6] had little effect on the specific activity of Fluc-EGFP but reduced the specific activity of FlucSM-EGFP and FlucDM-EGFP by ~20% and 50%, respectively (**Fig. 4a**). After treatment with MG132, we observed small, aggregate-like structures of Fluc-EGFP in ~25% of Fluc-EGFP–expressing cells, whereas ~70% of FlucSM-EGFP–expressing cells and ~90% of FlucDM-EGFP–expressing cells contained aggregates (**Fig. 4a**). This effect was apparently not caused by inhibition of degradation but rather by a general proteostasis imbalance, as the total cellular amount of sensor proteins detected by immunoblotting increased only slightly (**Supplementary Fig. 8**). Thus, Fluc mutants reported with high sensitivity on the impairment of proteostasis capacity resulting from Hsp90 or proteasome inhibition.

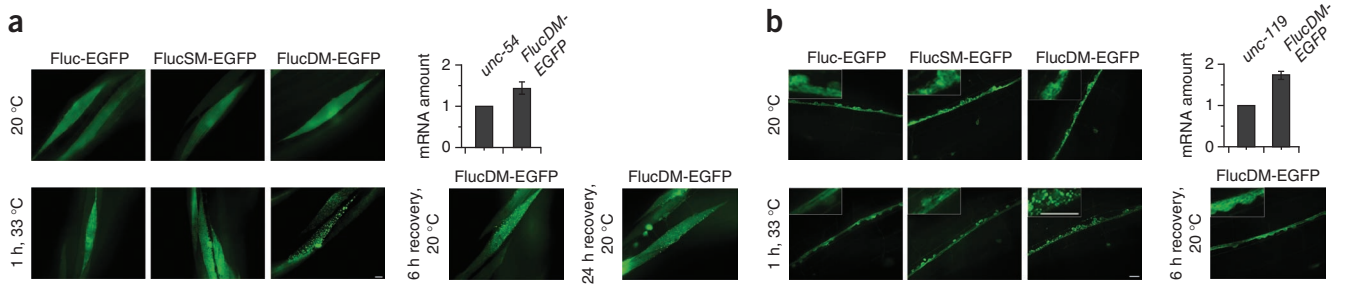

Figure 5 | Fluc-based sensors report on acute proteome stress during heat shock in *C. elegans*. (**a**,**b**) Representative fluorescence micrographs of young-adult worms (day 1) expressing Fluc-EGFP, FlucSM-EGFP or FlucDM-EGFP in body-wall muscle (**a**) or neuronal cells (**b**) under normal growth conditions at 20 °C, after heat stress for 1 h at 33 °C and after recovery at 20 °C for 6 h and 24 h (muscle-specific expression) or 6 h (neuron specific expression), as indicated. Scale bars, 10 μm. Insets in **b** show digitally magnified central regions of the respective images. Bar graphs show relative mRNA amounts of *FlucDM-EGFP*, muscle-specific *unc-54* (**a**) or neuron-specific *unc-119* (**b**) determined by RT-PCR. Error bars, s.d.; $n = 3$.

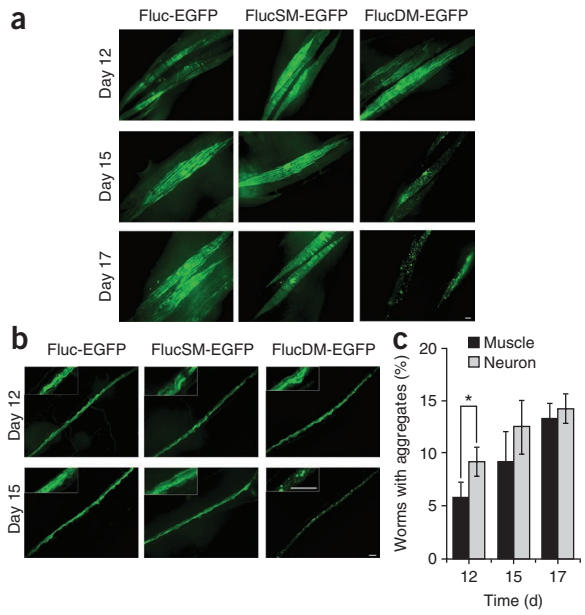

Figure 6 | Fluc-based sensors report on proteostasis decline during aging in *C. elegans*. (**a**,**b**) Fluorescence micrographs of worms expressing Fluc-EGFP, FlucSM-EGFP or FlucDM-EGFP in muscle (**a**) or neurons (**b**) imaged on indicated days. Scale bars, 10 µm. Insets show digitally magnified central region of the respective image. (**c**) FlucDM-EGFP–expressing worms containing aggregates on indicated days. Error bars, s.d.; $n = 3$. Forty worms were counted in each experiment. $^*P < 0.05$ (Student's *t*-test).

Proteostasis collapse by Huntington's disease protein

Expansion of a polyglutamine sequence in huntingtin protein is the cause of Huntington's disease, a neurodegenerative disorder associated with the formation of aggregates[21]. Overexpression of various chaperones can suppress polyglutamine toxicity and modulate aggregate formation[22]. Moreover, expression of polyglutamine-containing proteins in the nematode *C. elegans* results in the phenotypic expression of temperature-sensitive mutant alleles at the permissive temperature[8]. Thus, polyglutamine pathology is linked with proteostasis collapse.

To test whether Fluc-based sensors can be used to measure these changes in proteostasis, we transfected HEK293T cells with plasmids encoding the Fluc-EGFP variants and with *mCherry*-tagged huntingtin (*Htt*) exon 1 constructs encoding proteins with normal (20-glutamine; 20Q) or expanded (97-glutamine; 97Q) polyglutamine sequences. We observed large polyglutamine-containing aggregates 48 h after transfection in almost all cells expressing Htt-97Q, whereas Htt-20Q remained diffusely distributed (**Fig. 4b**). When we expressed Fluc-EGFP together with Htt-97Q, we observed small aggregate foci of Fluc-EGFP in only ~20% of the cells. But we detected multiple, more distinct foci in 50% of FlucSM-EGFP–expressing cells and observed massive aggregation of FlucDM-EGFP in 85% of the cells that also expressed Htt-97Q (**Fig. 4b**). In contrast, we did not detect aggregates in cells that expressed Fluc-EGFP variants and Htt-20Q (**Fig. 4b**). Aggregates of Fluc mutants and Htt-97Q were often located at different sites in the cell (**Fig. 4b**). Thus, the sensors confirmed findings in *C. elegans* that expression of polyglutamine expansion proteins results in a severe decline of cellular proteostasis[8].

Assessing proteostasis in *C. elegans*

We used *C. elegans* to test the Fluc mutants as proteostasis sensors in an organism. We expressed Fluc-EGFP variants in body-wall muscle cells using the *unc-54* promoter. Under normal growth conditions at 20 °C, the three sensor proteins had similar diffusely distributed expression in young adult worm (day 1). Upon heat stress (33 °C for 1 h), FlucDM-EGFP formed aggregates of various sizes that were dispersed throughout the cells, whereas Fluc-EGFP and FlucSM-EGFP remained diffusely distributed (**Fig. 5a**). Upon recovery from heat stress for at least 24 h, the number of aggregates was reduced and diffusely distributed EGFP fluorescence predominated, suggesting that the *C. elegans* muscle cells either resolubilized or disposed of the aggregates (**Fig. 5a**).

When we expressed the sensor proteins in neuronal cells using the *F25B3.3* promoter, we obtained similar results: upon heat-shock, FlucDM-EGFP formed aggregates whereas Fluc-EGFP and FlucSM-EGFP maintained diffuse distributions (**Fig. 5b**). During recovery, the aggregates of FlucDM-EGFP disappeared faster in neurons (within 6 h) than in muscle cells (24 h) (**Fig. 5b**), suggesting that in young worms neurons respond more efficiently to proteostasis imbalance than muscle cells. Reverse transcriptase–PCR (RT-PCR) experiments to quantify the expression of FlucDM-EGFP relative to unc-54 (muscle-specific) and unc-119 (neuron-specific) control proteins ruled out possible differences in sensor mRNA expression (**Fig. 5**).

Dysregulation of proteostasis during aging

Experiments in *C. elegans* have demonstrated a decline of proteostasis capacity during aging[5]. To test the utility of the Fluc-based sensors in monitoring this phenomenon, we analyzed distribution patterns of the proteins in muscle and neuronal cells of transgenic *C. elegans* throughout their adult lifespan. Muscle cells maintained diffuse distribution of Fluc-EGFP and FlucSM-EGFP until day 17, but small aggregates of FlucDM-EGFP became detectable by microscopy at day 12 and increased in number and size until day 17, with ~15% of the worms containing distinct aggregates (**Fig. 6**). In neurons, aggregates of FlucDM-EGFP tended to occur more frequently already at days 12 and 15 (**Fig. 6b**,**c**). Thus, although in young-adult worms, neuronal cells respond more efficiently to acute stress than muscle (**Fig. 5b**), they appeared to be less capable of maintaining proteostasis during chronic proteome stress during aging.

DISCUSSION

Deficiency in cellular proteostasis capacity has been suggested as a cause or a consequence of many diseases in which key proteins misfold and aggregate, giving rise to loss-of-function and toxic gain-of-function effects[1]. Many of these diseases affect preferentially the elderly, which is consistent with a gradual loss of proteostasis during aging[23].

The Fluc-based sensors we developed can be used at 20–37 °C, with the more destabilized FlucDM reporting on proteostasis at 20 °C, the normal growth temperature of *C. elegans*. The folding state of these proteins can be readily estimated via their specific enzymatic activity. A key advantage is that the sensors have no biological function in the experimental systems of interest, and thus their misfolding in conditions of proteostasis deficiency is not associated with loss-of-function effects. Low expression levels are sufficient to follow the luminescence-based sensor activity and EGFP fluorescence, thus minimizing effects on proteostasis by the sensors themselves.

The Fluc-based sensors formed cytosolic foci during heat stress that disappeared partially during recovery. Analysis of this process in *C. elegans* revealed notable differences between muscle and neuronal cells in the capacity to remove aggregates of stress-denatured proteins and to maintain the proteins soluble during normal aging, consistent with recent observations[24]. Moreover, the sensor proteins aggregated when proteostasis was compromised in human cells as a result of the expression of polyglutamine-expanded huntingtin. The luciferase proteins were often deposited in aggregate structures distinct from those of the polyglutamine protein, and thus should prove useful as tools in the cell biological and biochemical analysis of aggregation pathways for different types of proteins[25]. Stable cell lines or transgenic *C. elegans* lines expressing the reporters may be used to explore various aspects of the proteostasis machinery by high-throughput screening. As demonstrated with the Hsp90 inhibitor 17-AAG and the proteasome inhibitor MG132, the effect of small-molecule compounds on the status of the proteostasis network can easily be measured using the Fluc-based sensors. Thus, chemical screens for proteostasis-regulating compounds that improve the activity of the sensor proteins may be designed.

The sensors we describe report mainly on cytosolic proteome stress. However, by attaching appropriate signals for subcellular targeting, it is possible to generate sensors selectively measuring proteostasis capacity in different membrane compartments, such as the endomembrane system, nucleus and mitochondria. Reporter cell lines simultaneously expressing two or more of these sensors, carrying different fluorescent tags, may be used to directly compare the fate of differentially destabilized proteins. The extent to which the Fluc-based sensors can monitor the full range of proteostasis-related functions in mammalian cells remains to be explored. A careful comparison of their behavior with that of endogenous proteins of different structural classes will be useful for validation.

METHODS

Methods and any associated references are available in the online version of the paper at http://www.nature.com/naturemethods/.

Note: Supplementary information is available on the Nature Methods website.

ACKNOWLEDGMENTS

We thank M. Hipp, Y.E. Kim and M. Hayer-Hartl for discussion, F. Buchholz (Max Planck Institute for Molecular Cell Biology and Genetics) for providing Hsc70 endoribonuclease-prepared small interfering (esi)RNA, and H. Wagner (Institut für Med. Mikrobiologie, Immunologie und Hygiene, Technische Universität München) for the HSP70-Luc plasmid. We acknowledge the expert technical assistance of V. Marcus. This work has been supported by the European Commission within the 7th framework program Proteomics Specification in Time and Space.

AUTHOR CONTRIBUTIONS

S.R. and F.U.H. conceived the idea and developed the method. A.B. designed Fluc mutants. R.G., C.L. and S.R. performed molecular biology and cell biology experiments. P.K. and M.Z. performed *C. elegans* experiments. A.V. and D.G. performed *D. melanogaster* S2 cell experiments. R.G. and S.R. analyzed results. S.R. and F.U.H. interpreted results and wrote the manuscript with assistance from D.G.

COMPETING FINANCIAL INTERESTS

The authors declare competing financial interests: details accompany the full-text HTML version of the paper at http://www.nature.com/naturemethods/.

Published online at http://www.nature.com/naturemethods/.
Reprints and permissions information is available online at http://www.nature.com/reprints/index.html.

1. Powers, E.T., Morimoto, R.I., Dillin, A., Kelly, J.W. & Balch, W.E. Biological and chemical approaches to diseases of proteostasis deficiency. *Annu. Rev. Biochem.* **78**, 959–991 (2009).
2. Vabulas, R.M., Raychaudhuri, S., Hayer-Hartl, M. & Hartl, F.U. Protein folding in the cytoplasm and the heat shock response. *Cold Spring Harb. Perspect. Biol.* **2**, a004390 (2010).
3. Frydman, J. Folding of newly translated proteins *in vivo*: the role of molecular chaperones. *Annu. Rev. Biochem.* **70**, 603–647 (2001).
4. Rubinsztein, D.C. The roles of intracellular protein-degradation pathways in neurodegeneration. *Nature* **443**, 780–786 (2006).
5. Ben-Zvi, A., Miller, E.A. & Morimoto, R.I. Collapse of proteostasis represents an early molecular event in *Caenorhabditis elegans* aging. *Proc. Natl. Acad. Sci. USA* **106**, 14914–14919 (2009).
6. Balch, W.E., Morimoto, R.I., Dillin, A. & Kelly, J.W. Adapting proteostasis for disease intervention. *Science* **319**, 916–919 (2008).
7. Mu, T.W. *et al.* Chemical and biological approaches synergize to ameliorate protein-folding diseases. *Cell* **134**, 769–781 (2008).
8. Gidalevitz, T., Ben-Zvi, A., Ho, K.H., Brignull, H.R. & Morimoto, R.I. Progressive disruption of cellular protein folding in models of polyglutamine diseases. *Science* **311**, 1471–1474 (2006).
9. Frydman, J., Nimmesgern, E., Ohtsuka, K. & Hartl, F.U. Folding of nascent polypeptide chains in a high molecular mass assembly with molecular chaperones. *Nature* **370**, 111–117 (1994).
10. Thulasiraman, V. & Matts, R.L. Effect of geldanamycin on the kinetics of chaperone-mediated renaturation of firefly luciferase in rabbit reticulocyte lysate. *Biochemistry* **35**, 13443–13450 (1996).
11. Nimmesgern, E. & Hartl, F.U. ATP-dependent protein refolding activity in reticulocyte lysate. Evidence for the participation of different chaperone components. *FEBS Lett.* **331**, 25–30 (1993).
12. Schroder, H., Langer, T., Hartl, F.U. & Bukau, B. DnaK, DnaJ and GrpE form a cellular chaperone machinery capable of repairing heat-induced protein damage. *EMBO J.* **12**, 4137–4144 (1993).
13. Conti, E., Franks, N.P. & Brick, P. Crystal structure of firefly luciferase throws light on a superfamily of adenylate-forming enzymes. *Structure* **4**, 287–298 (1996).
14. Naylor, L.H. Reporter gene technology: the future looks bright. *Biochem. Pharmacol.* **58**, 749–757 (1999).
15. Hageman, J., Vos, M.J., van Waarde, M.A. & Kampinga, H.H. Comparison of intra-organellar chaperone capacity for dealing with stress-induced protein unfolding. *J. Biol. Chem.* **282**, 34334–34345 (2007).
16. Michels, A.A., Nguyen, V.T., Konings, A.W., Kampinga, H.H. & Bensaude, O. Thermostability of a nuclear-targeted luciferase expressed in mammalian cells. Destabilizing influence of the intranuclear microenvironment. *Eur. J. Biochem.* **234**, 382–389 (1995).
17. Matsui, I. & Harata, K. Implication for buried polar contacts and ion pairs in hyperthermostable enzymes. *FEBS J.* **274**, 4012–4022 (2007).
18. Schneider, C. *et al.* Pharmacologic shifting of a balance between protein refolding and degradation mediated by Hsp90. *Proc. Natl. Acad. Sci. USA* **93**, 14536–14541 (1996).
19. Sharp, S. & Workman, P. Inhibitors of the HSP90 molecular chaperone: current status. *Adv. Cancer Res.* **95**, 323–348 (2006).
20. Taipale, M., Jarosz, D.F. & Lindquist, S. HSP90 at the hub of protein homeostasis: emerging mechanistic insights. *Nat. Rev. Mol. Cell Biol.* **11**, 515–528 (2010).
21. Muchowski, P.J. Protein misfolding, amyloid formation, and neurodegeneration: a critical role for molecular chaperones? *Neuron* **35**, 9–12 (2002).
22. Broadley, S.A. & Hartl, F.U. The role of molecular chaperones in human misfolding diseases. *FEBS Lett.* **583**, 2647–2653 (2009).
23. Morimoto, R.I. & Cuervo, A.M. Protein homeostasis and aging: taking care of proteins from the cradle to the grave. *J. Gerontol. A Biol. Sci. Med. Sci.* **64**, 167–170 (2009).
24. Kern, A., Ackermann, B., Clement, A.M., Duerk, H. & Behl, C. HSF1-controlled and age-associated chaperone capacity in neurons and muscle cells of *C. elegans*. *PLoS ONE* **5**, e8568 (2010).
25. Kaganovich, D., Kopito, R. & Frydman, J. Misfolded proteins partition between two distinct quality control compartments. *Nature* **454**, 1088–1095 (2008).
26. Nakatsu, T. *et al.* Structural basis for the spectral difference in luciferase bioluminescence. *Nature* **440**, 372–376 (2006).

ONLINE METHODS

Availability of materials. Sensors are available from the authors upon request.

Generation of expression constructs. The luciferase gene from plasmid pGL3 basic (Promega) encoding residues 1–550 of wild-type Fluc (with the C-terminal peroxisomal targeting signal Ser-Lys-Leu replaced by Ile-Ala-Val and containing two point mutations, Asn50Asp and Asn119Gly, to improve efficiency of the enzyme) was PCR-amplified and sub-cloned into the pCIneo vector (Promega) to form pCIneoFluc. Site-directed mutagenesis was performed to introduce the desired mutations by routine protocol. Briefly, the pCIneoFluc vector was PCR-amplified using Pfu polymerase (Promega) with specific site-directed mutagenesis primers (**Supplementary Table 1**); the PCR product was treated with DpnI, and transformed into competent *Escherichia coli*. Constructs were routinely sequenced to confirm the mutations. pCIneoFluc constructs were used for *in vitro* translation in rabbit reticulocyte lysate (RRL) and for expression in mammalian cell culture.

To prepare EGFP-tagged constructs, the stop codon of the luciferase gene in the pCIneoFluc was changed to AAA, encoding lysine. *EGFP* from the pEGFP-N2 vector (Clontech) was inserted at the 3′ end of *luciferase* using XmaI and NotI restriction sites to form pCIneoFluc-EGFP. EGFP-tagged luciferase variants were cloned for *C. elegans* studies in a similar manner in the pPD30-38 vector (under the *unc-54* promoter) for muscle-specific expression and in pDP#SU006 (under the *F25B3.3* promoter) for neuron-specific expression.

Huntingtin constructs were prepared by cloning the exon 1 fragment of the huntingtin gene containing sequence encoding the polyglutamine region (20-Gln or 97-Gln)[27] N-terminally fused to mCherry in the pCDNA3.1(+) mammalian expression vector (Invitrogen) using BamHI and XhoI restriction sites. All constructs were verified by sequencing.

To generate the construct *HSPA1A-Renilla-myc*, expressing C-terminally Myc-tagged Rluc under control of the *HSPA1A* promoter, the *Rluc* gene was PCR-amplified from the phRL-TK vector (Promega) and subcloned into plasmid *HSP70-Luc* (*Fluc* gene under control of the HSF1-dependent *HSPA1A* promoter, gift from H Wagner) replacing the *Fluc* gene using XhoI and FseI. A *myc* tag was introduced at the 3′ end of the *Rluc* gene by sequential site-directed mutagenesis.

***In vitro* characterization of luciferase mutants.** Luciferase mutants were transcribed and translated at 30 °C in RRL using the Promega TnT T7 quick coupled transcription and translation kit according to the guidelines of the manufacturer. To analyze the functional stability of the mutant proteins, translation reactions were stopped by threefold dilution of samples into ice-cold buffer A (25 mM Tris-phosphate (pH 7.8), 2 mM trans-1, 2-cyclo-hexanediaminetetraacetate (CDTA) and 1 mg ml^{-1} BSA) containing 2 mM cycloheximide. The reactions were incubated at various temperatures, and luciferase activity was determined at the indicated times. To determine specific activities (luciferase activity normalized to the luciferase protein content in the sample), aliquots were withdrawn and analyzed by immunoblotting with Fluc antibody (Promega G7451, polyclonal, which recognizes wild-type and mutant luciferase proteins with similar efficiency). To assess the structural flexibility of Fluc variants, aliquots of translation reactions diluted as above were incubated in the presence or absence of proteinase K (1 μg ml^{-1}) (Merck) for the indicated times at 20 °C, followed by addition of 5 mM PMSF to inhibit proteinase K action. The pattern of proteinase K digestion was visualized by immunoblotting with Fluc antibody. All antibodies and reagents used in this study to characterize Fluc mutants are described in **Supplementary Tables 2** and **3**.

Cell culture and transfection. HeLa and HEK293T cells were maintained in Dulbecco's Modified Eagle's medium (DMEM; Biochrom) supplemented with 10% FBS (Gibco), 1% penicillin-streptomycin (Gibco) and 1% L-glutamine (Gibco) at 37 °C in an atmosphere of 5% CO_2. To perform heat-stress experiments, cells were transiently transferred to an incubator at 43 °C. Cells were transiently transfected using Lipofectamine and PLUS reagent (Invitrogen) according to the manufacturer's protocol. We used 1 μg of DNA for transfection in 12-well format. esiRNA reverse-transfection experiments were performed with Lipofectamine RNAiMAX (Invitrogen). We used 300 ng of esiRNA for transfection in 12-well format. Forty-eight hours after esiRNA transfection, cells were again transfected with Fluc constructs as described above.

To prepare total cell protein for immunoblotting, cells were boiled in SDS sample buffer or dissolved in SDT buffer (4% (w/v) SDS, 100 mM Tris-HCl (pH 7.6) and 0.1 M DTT). To prepare soluble cell fractions, cells were trypsinized and washed twice with PBS. Cells were then pelleted and resuspended in lysis buffer (50 mM Tris (pH 7.8), 150 mM NaCl, 1% (v/v) NP-40, 0.25% sodium deoxycholate, 1 mM EDTA and 1 tablet protease inhibitor cocktail (Roche) per 10 ml) and vortexed at regular intervals for 40 min on ice. The crude cell lysate was then centrifuged at 16,100*g* for 30 min at 4 °C. The supernatant fraction was used for analysis of soluble luciferase protein amount. Pellets were dissolved in SDT buffer.

For Fluc activity measurements, ~10,000 cells were seeded in 96-well plates in 100 μl DMEM. After 24 h, the cells were lysed by adding 50 μl of Steady-Glo Luciferase Assay system buffer (Promega) directly to the wells and incubated for 15 min in the dark at room temperature (25 °C). Luminescence was then recorded in a luminometer (Berthold Lumat LB9507) (acquisition time, 2 s).

To determine relative specific luciferase activities, luciferase luminescence values were divided by luciferase band intensities (generally in total, SDS-solubilized cells or in soluble fractions when indicated) quantified from immunoblots by densitometry using the Advanced Image Data Analyzer (AIDA version 4.15.025).

Protocols for experiments in *Drosophila* S2 cells are described in **Supplementary Note 1**.

Generation of transgenic *C. elegans*. Nematodes were maintained using standard procedures at 20 °C. Transgenic *C. elegans* were generated by microinjection. Fluc-EGFP expression vectors (25 μg ml^{-1}) together with the injection marker pRF4 (rol-6 (su1006), 125 μg ml^{-1}) were injected into the gonads of adult wild-type hermaphrodite worms. Transgenic F1 progeny were selected on the basis of the roller phenotype. Individual transgenic F2 worms that were rollers with fluorescence were picked to establish independent lines. To achieve chromosomal integration, selected extrachromosomal lines were UV-light irradiated

at an energy of 300 J and integrated strains were backcrossed six times before using them in experiments.

RT-PCR experiments in *C. elegans*. Total RNA was isolated from ~600 FlucDM-EGFP–expressing worms by the trizol method, and 1 µg of RNA was converted to cDNA using the iScript Select cDNA Synthesis Kit (Bio-Rad). PCR amplification was carried out in 25 cycles using three different dilutions of cDNA in 50 µl reaction volume; 5 µl of amplified product was analyzed on 2% agarose gels. Experiments were repeated at least three times, and band intensities were quantified using AIDA image analyzer software. The primers used in this experiment are described in **Supplementary Table 1**.

Fluorescence microscopy. Mammalian cells were grown on coverslips, fixed with 4% paraformaldehyde, washed with PBS, stained with DAPI and mounted on slides for microscopy. Worms were fixed in ethanol and mounted on slides using Dako fluorescent mounting medium. Fluorescence imaging was performed on a Zeiss Axiovert 200M fluorescence microscope equipped with a Zeiss Axiocam HRM camera. The filter sets used to capture the images were the following: for DAPI, filter set 1 (beam splitter FT395, excitation filter BP365/12, emission filter LP397); for EGFP, filter set 38 (beam splitter FT580, excitation filter BP470/40, emission filter BP525/50); and for cy3/mCherry, filter set15 (beam splitter FT495, excitation filter BP546/12, emission filter LP590). Images were taken using Axiovision Rel 4.7 software. Images were resized and brightness and contrast was adjusted in Adobe Photoshop CS3. Figures were prepared in Adobe Illustrator CS3.

27. Behrends, C. *et al.* Chaperonin TRiC promotes the assembly of polyQ expansion proteins into nontoxic oligomers. *Mol. Cell* **23**, 887–897 (2006).

doi:10.1038/nmeth.1697